Electroproduction of Strangeness and Spectroscopy of Hypernuclei

M. Sotona
Nuclear Physics Institute, Prague

Hypernuclear spectroscopy - hyperon - nucleon residual interaction, Λ behavior in nuclear environment, ...

Hypernuclear spectroscopy on meson end photon beams

$$a + A \Rightarrow b + HN$$

$(K^-, \pi^-), (\pi^+, K^+), (K^-_{stopped}, \pi^-), (\gamma, K^+)$, reactions
Distorted Wave Impulse Approximation (DWIA) :

$$d\sigma \sim |T_{if}|^2 d\vec{p}_b \; d\vec{P}_{HN}$$

$$T_{if} \sim \sum_N \langle \Psi_b \Psi_{HN} | (b, \Lambda | t | a, N) | \Psi_a \Psi_A \rangle \qquad (1)$$

Ψ_A, Ψ_{HN} - target (ground state) and hypernucleus many-particle wave functions (shell model)

Ψ_a, Ψ_b - meson wave functions (distorted waves, optical potential, eikonal approximation)

$(b, \Lambda | t | a, N)$ - t-matrix of elementary process or hadron current for reaction on individual nucleons

- Production cross section - strong dependence on momentum transferred to HN $q_{tr} = |\vec{p}_a - \vec{p}_b|$ $\Rightarrow$ small pion, kaon scattering angles !!

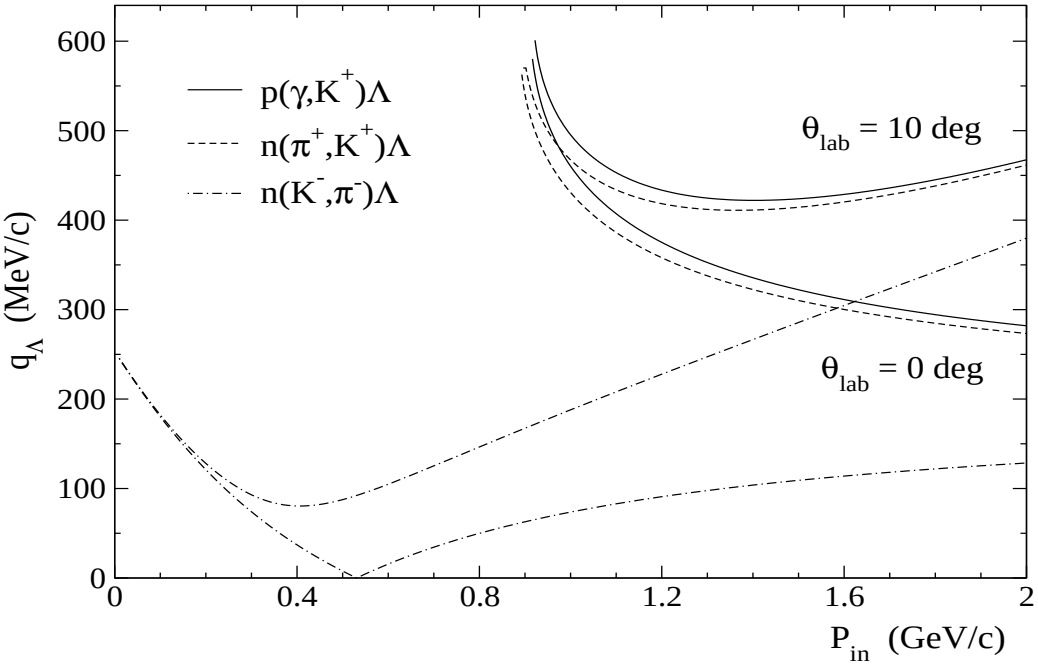

Figure 1: Momentum transfer in various strangeness production reactions.

- non-spin flip versus spin flip

  K, π - pseudoscalar mesons $J^\pi = O^-$ - reaction amplitude

$$F = f(s,t) + ig(s,t)(\vec{\sigma}.\vec{n}, \vec{n} = \frac{\vec{p}_a \times \vec{p}_b}{|\vec{p}_a \times \vec{p}_b|}$$

  non-spin-flip (f) and spin-flip (g) term.

  photons (real or virtual)

$$J^i_{\rm lab} = F_1(s,t)\sigma^i + iF_2(s,t)(\hat{q} \times \hat{p}_K)^i + F_3(s,t)(\vec{\sigma}\hat{q})\hat{p}^i_K + F_4(s,t)(\vec{\sigma}\hat{p}_K)\hat{p}^i_K +$$
$$F_5(s,t)(\vec{\sigma}\hat{q})\hat{q}^i + F_6(s,t)(\vec{\sigma}\hat{p}_K)\hat{q}^i, \quad i = 0, \pm 1.$$

spin flip terms dominant

(K^-, π^-) - $q_{tr} < k_F$, only $\Delta L = \Delta J = 0$, substitutional states

(π^+, K^+) - $q_{tr} > k_F$, $\Delta L = \Delta J = 1, 2$ HN

(γ, K^+) – $q_{tr} > k_F$, strong spin flip – $\Delta L = 1, 2,\ \Delta S = 1,\ \Delta J = 1, 2, 3$ states populated

Description of electro-production process

The kinematics of the electroproduction reaction

$$e(p_e) + p/A(p_p/p_A) \rightarrow e'(p_e^{'}) + K^+(p_K) + \Lambda/HN(p_\Lambda/p_{HN})$$

on proton(p) or nuclear(A) target producing Λ hyperon or hypernucleus(HN) respectively is depicted in Fig.

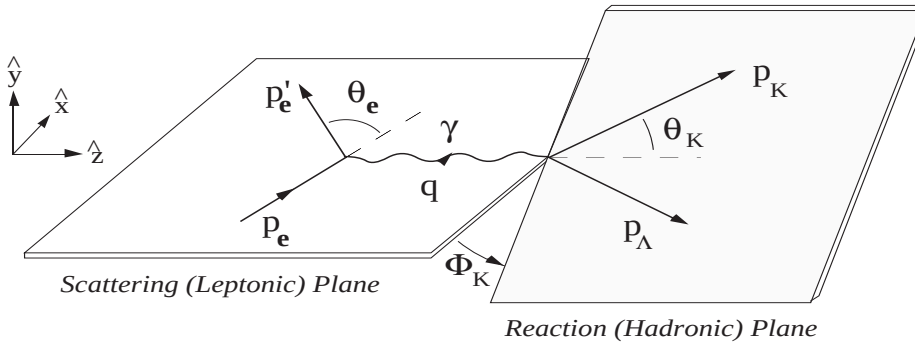

Figure 2: Kinematics of an electroproduction process.

To establish notation, the particle four-momenta are given in parentheses . Four-momentum transferred to the nucleon $q = \{\omega, \vec{q}\}$ (*virtual photon four-momentum*) is defined by $\omega = E_e - E_e^{'}, \vec{q} = \vec{p}_e - \vec{p}_e^{\,'}$. *"Virtuality"* of exchanged photon is determined by its (nonzero) four-momentum square q^2. This photon is space-like ($q^2 < 0$) and for this reason the positive quantity $Q^2 = -q^2$ is usually used in the literature:

$$Q^2 = \vec{q}^{\,2} - \omega^2 = 2(E_e E_e^{'} - m_e^2 - \mid \vec{p}_e \mid\mid \vec{p}_e^{\,'} \mid \cos\theta_e)$$

.

The triple differential cross section may then be expressed as a product of two terms, virtual photon flux Γ and the photoproduction cross section by virtual photons:

$$\frac{d^3\sigma}{dE_e' d\Omega_e' d\Omega_K} = \Gamma \frac{d\sigma}{d\Omega_K},$$

$$\frac{d\sigma}{d\Omega_K} = \frac{d\sigma_T}{d\Omega_K} + \epsilon_L \frac{d\sigma_L}{d\Omega_K} + \epsilon \frac{d\sigma_{TT}}{d\Omega_K} - \frac{Q^2}{\omega^2} l^s_{xz} \frac{d\sigma_{TL}}{d\Omega_K} - h \left\{ \frac{Q^2}{\omega^2} l^a_{yz} \frac{d\sigma_{TL'}}{d\Omega_K} - l^a_{xy} \frac{d\sigma_{TT'}}{d\Omega_K} \right\}.$$

Electroproduction on complex nuclear target

It is quite natural to suppose that in the one-photon-exchange approximation the transition amplitude of the electroproduction process Eq. (1) *at complex nuclear target* can be written again as the invariant product of leptonic and hadronic currents mediated by the virtual photon propagator Eq. (4). Now, however, the hadron current is *many-particle operator* dependent on the internal structure of target nucleus and produced hypernucleus.

Distorted wave impulse approximation (DWIA) was successfully used to describe hypernuclear production in $(K^-, \pi^-), (\pi^+, K^+)$ and $(K^-_{stopped}, \pi^-)$ reactions. Rather high particle momenta ($\mid \vec{q} \mid, \mid \vec{p}_K \mid \simeq 1\ GeV$) involved in the electroproduction reaction justify an assumption that one can apply $DWIA$ also in this case. The simple matrix element of single-particle hadron current in the transition matrix must be therefore substituted by the corresponding many-particle matrix element between the (nonrelativistic) nuclear and the hypernuclear wave functions

$$T^{if}_k \ = \ \langle \Psi_H | \ \sum_{j=1}^{Z} \ \chi_\gamma \ \chi^*_K \ J_k(p_\Lambda \ p_K, p^j_p \ q) \ | \Psi_A \rangle, \quad k = x, y, z.$$

The sum runs over the Z target protons and $\Psi_A(\Psi_H)$ is the many-particle (shell-model) wave function of target nucleus (hypernucleus). Virtual photon four-momentum $q = p_e - p'_e$, $p_p(p_\Lambda)$ are four-momenta of (bound) proton and hyperon. The quantity χ_γ is the virtual photon wave function (the product of the wave functions of incoming and outgoing electrons in the plane wave approximation - the Coulomb distortion is neglected for relativistic electrons). The kaon distorted wave χ_K is calculated in the optical potential model.

Important items of the calculation:

1. Ψ_A, Ψ_{HN} - target (ground state) and hypernucleus many-particle wave functions (shell model - see John Millener contribution)

2. Ψ_a, Ψ_b - meson wave functions (distorted waves, optical potential, eikonal approximation)

   First order optical potential

$$V_{opt} \sim \sigma_{tot}\{i - \frac{Ref}{Imf}\}\rho(r)$$

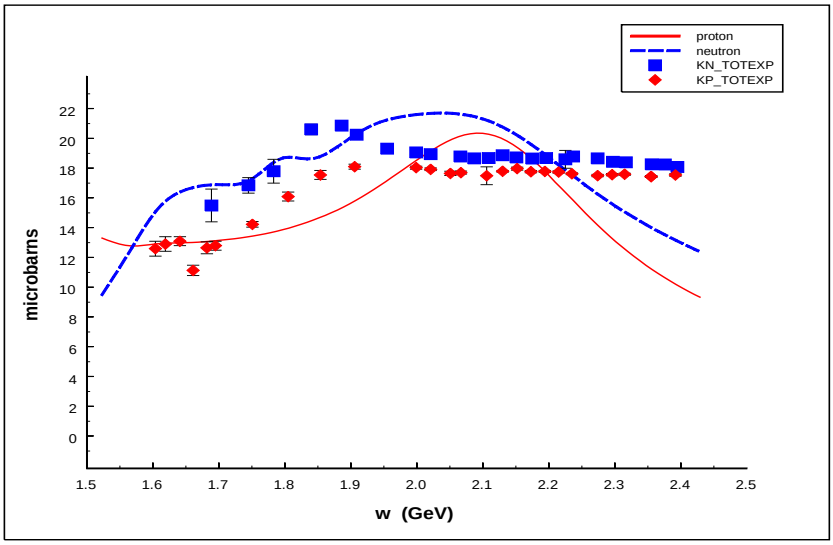

Figure 3: KN total cross section.

   Real part - from Martin or other parametrization of KN data.

3. model of hadron current for elementary process

$$J^i_{\rm lab} = F_1(s,t)\sigma^i + iF_2(s,t)(\hat{q}\times\hat{p}_K)^i + F_3(s,t)(\vec{\sigma}\hat{q})\hat{p}^i_K + F_4(s,t)(\vec{\sigma}\hat{p}_K)\hat{p}^i_K +$$
$$F_5(s,t)(\vec{\sigma}\hat{q})\hat{q}^i + F_6(s,t)(\vec{\sigma}\hat{p}_K)\hat{q}^i, \quad i = 0, \pm 1.$$

because the cross section of elementary and many-particle process depend in principle on various combinations of six amplitudes involved and the models predicted the "same" cross sections and polarizations of elementary reaction can result in different predictions for the hypernuclear production

$^{12}C(e,e'K^+)^{12}B_\Lambda$ reaction, E89-009 Hall C experiment

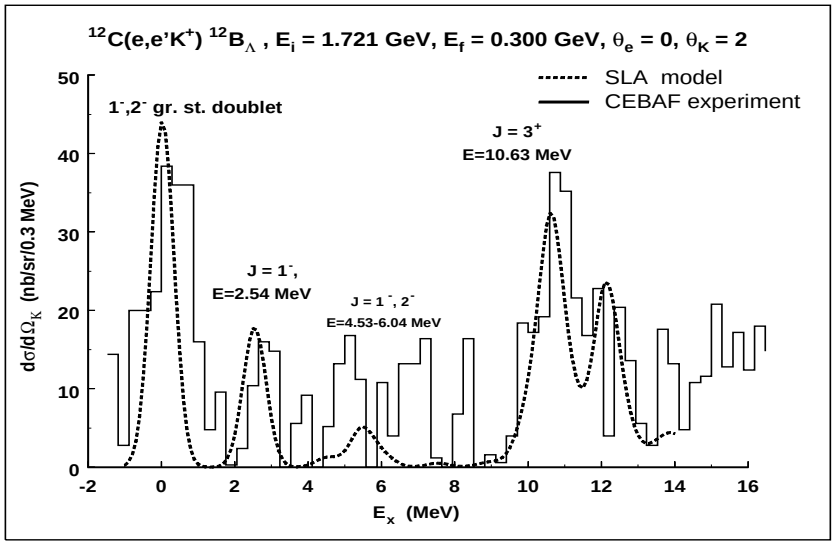

Figure 4: E 89-009 JLab experiment

Model dependence

Table 1: Differential cross section for $^{12}C(e,e'K^+)^{12}B_\Lambda$ reaction at kaon scattering angle $\Theta_{K\gamma} = 2.$ and different electroproduction models

model	$E \simeq 0\ MeV$	$E = 2.54\ MeV$	$E \sim 5.5\ MeV$
AS2	123.7	49.4	16.9
WJC2	166.8	67.4	23.1
WJC3	107.6	42.9	14.8
WJC4	180.8	72.8	25.1
WJC1	143.5	57.2	19.7
AB1	138.9	55.5	19.1
SLA	140.7	56.9	19.5
KMAID	99.0	38.7	14.4
Exper.	$140 \pm 17 \pm 18$	$59 \pm 14 \pm 7$	$30 \pm 15 \pm 4$

We demonstrated that *Distorted Wave Impulse approximation* in standard form together with modern photoproduction models (Saclay - Lyon) is able to describe first hypernuclear electroproduction data taken on ^{12}C target reasonably well

E 94 - 107 Hall A experiment - ^{12}C target

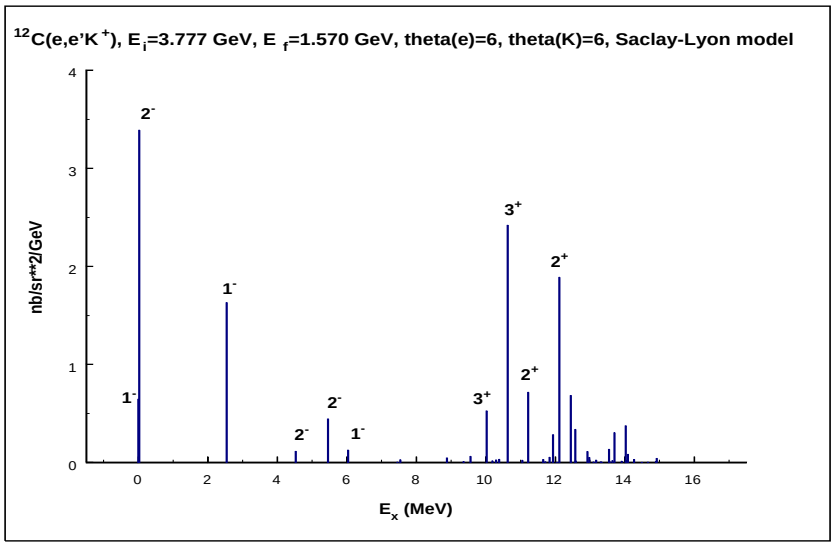

Figure 5: Contribution of individual HN levels

What we can learn from the comparison of $^{12}C_\Lambda$ and $^{12}B_\Lambda$?

Λ binding energy $B_\Lambda = 10.8\ MeV(^{12}C_\Lambda), 11.37\ MeV(^{12}B_\Lambda)$ - *charge symmetry breaking in* $\Lambda - N$ *interaction or some problem with photoemulsion* B_Λ *value for* $^{12}C_\Lambda$ *??*

E 94 - 107 Hall A experiment - ^{16}O target

Schematic picture of expected energy spectra:

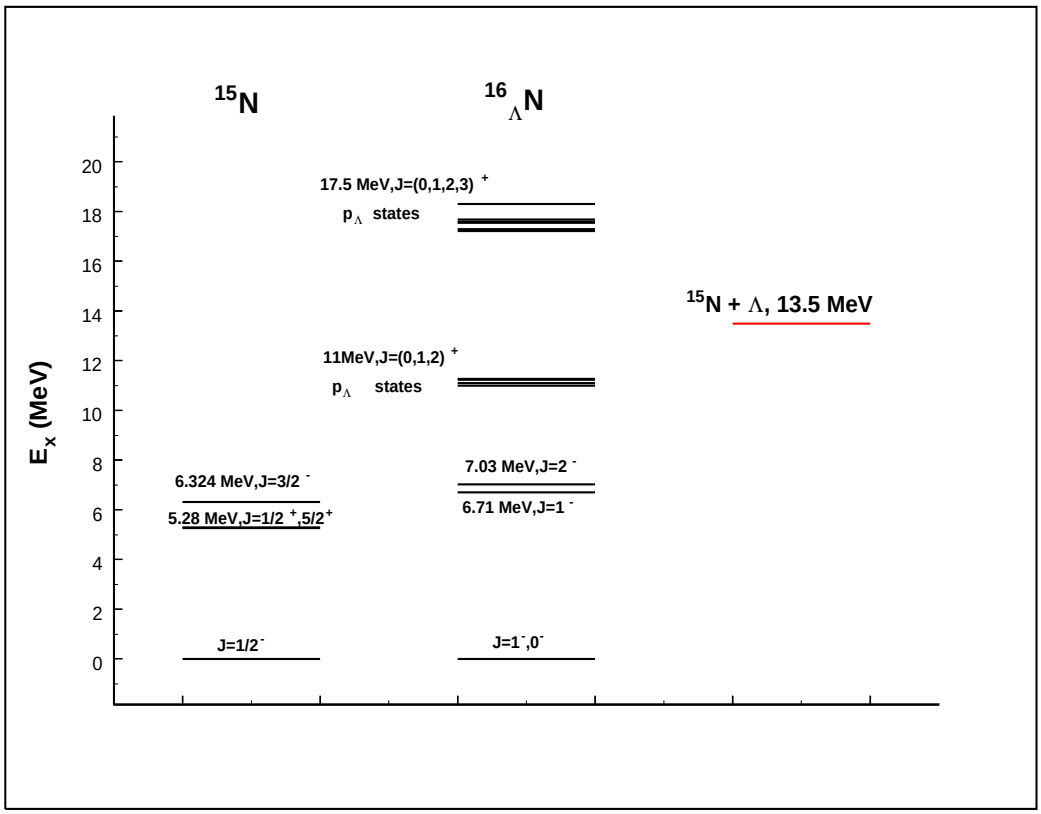

Figure 6:

Contribution of individual levels

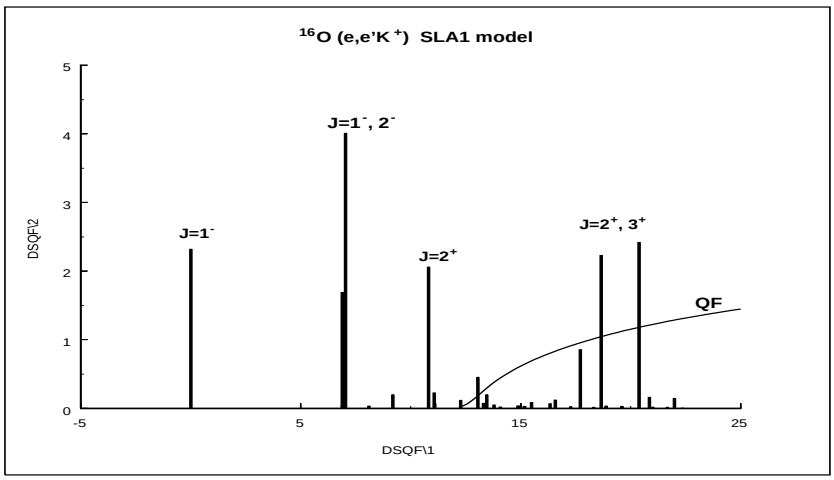

Figure 7: Contribution of individual HN levels

E 94 - 107 Hall A experiment - ^9Be target

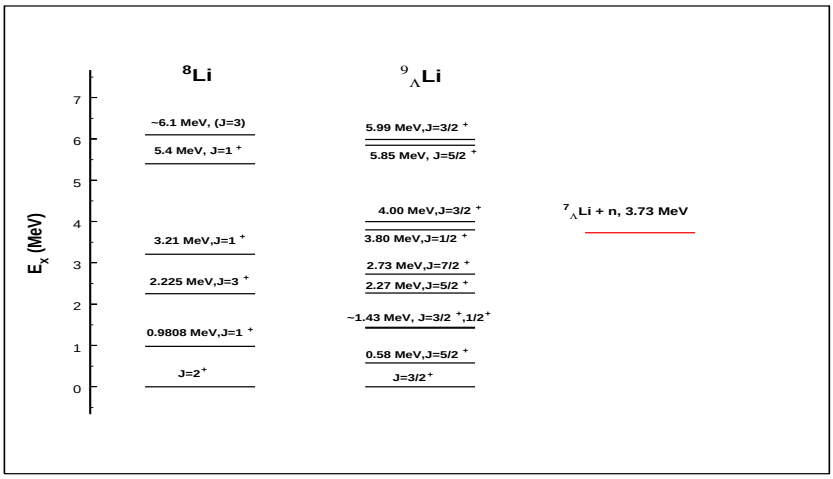

Figure 8: Calculated energy spectra - John Millener

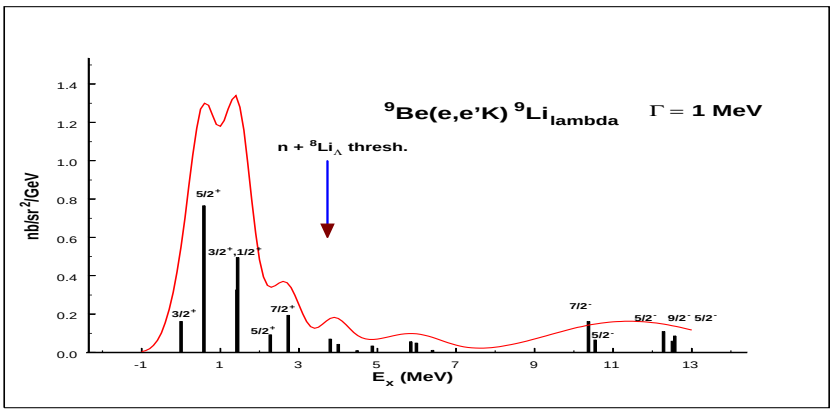

Figure 9: Calculated cross sections

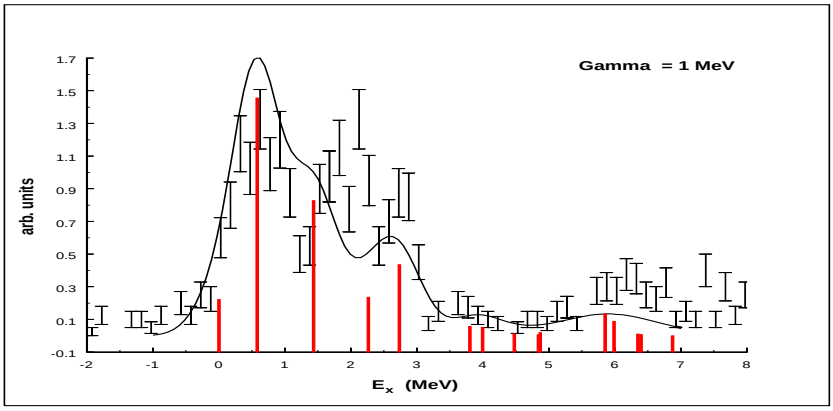

Figure 10: Calculated versus experimental cross section

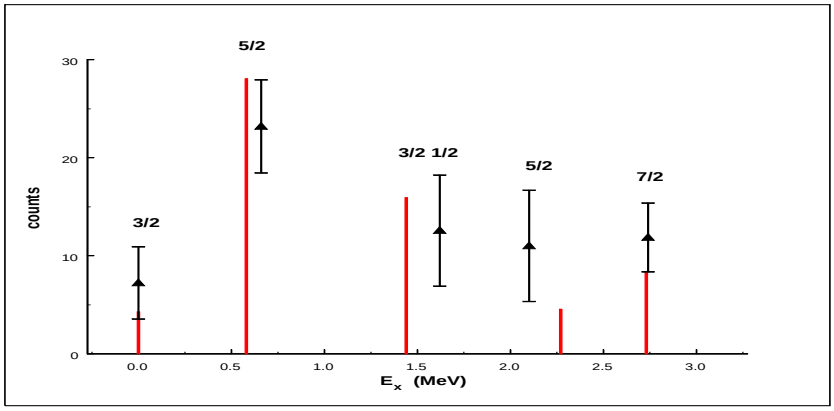

Figure 11: Comparison of theoretical predictions and experimental data.

^{208}Pb target - very preliminary

Assumptions: ^{208}Pb target - neutron and proton closed shells. Core ^{207} core nucleus - simple proton holes

Cross section at Hall A kinematics

at the same kinematics the cross section for hypernuclear production on carbon and oxygen target is typically approx. 1 to 3 nonobarns

Table 2: ^{207}Tl energy spectrum, dominant configurations and spectroscopic factors

E_x MeV	J^π	Config.	C^2S
0.000	$1/2+$	$2s^{-1}_{1/2}$	1.70
0.351	$3/2^+$	$1d^{-1}_{3/2}$	3.58
1.348	$11/2^-$	$0h^{-1}_{11/2}$	10.6
1.683	$5/2^+$	$1d^{-1}_{5/2}$	3.75
—	—	—	—
3.747	$7/2^+$	$0g^{-1}_{7/2}$	2.17

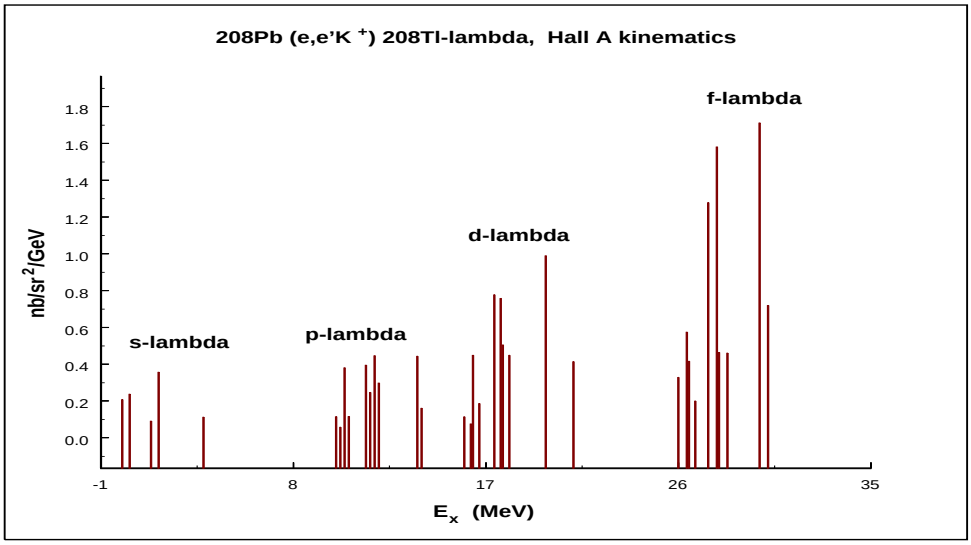

Figure 12: Cross section estimates of hypernuclear electroproduction on 208Pb target